ISSN 1070-3284, Russian Journal of Coordination Chemistry, 2009, Vol. 35, No. 5, pp. 320–329. © Pleiades Publishing, Ltd., 2009.
Original Russian Text © O.R. Simonova, S.V. Zaitseva, O.I. Koifman, 2009, published in Koordinatsionnaya Khimiya, 2009, Vol. 35, No. 5, pp. 326–335.

Influence of Imidazole on the Kinetics of Oxidation of 5,15-Di(*ortho*-methyloxyphenyl)-2,3,7,8,12,13,17,18-octamethylporphyrin with Organic Peroxides in *o*-Xylene

O. R. Simonova[a], S. V. Zaitseva[a], and O. I. Koifman[a,b]

[a] *Institute of Solution Chemistry, Russian Academy of Sciences, ul. Akademicheskaya 1, Ivanovo, 153045 Russia*

[b] *Ivanovo State University of Chemical Technology, Ivanovo, Russia*

E-mail: ors@isc-ras.ru

Received July 9, 2008

Abstract—The structure of zinc 5,15-di(*ortho*-methyloxyphenyl)-2,3,7,8,12,13,17,18-octamethylporphyrin was studied by spectrophotometry and computer simulation. Its properties in the reaction with organic peroxides in *o*-xylene in the presence of imidazole were studied at 295 K. The apparent and true rate constants for this process were calculated. The metalloporphyrin chromophore was found to decompose completely during the interaction of the zinc porphyrin (ZnP) with peroxides. The influence of imidazole on the reaction rate was revealed. The geometric characteristics of the optimized ZnP structure and intermediates of the oxidation were obtained by the PM3 quantum-chemical method. The deformational strains in the ZnP macrocycle were found to increase during the reaction.

DOI: 10.1134/S1070328409050029

INTRODUCTION

Porphyrins and their metallocomplexes are representatives of a large class of intracomplex compounds characterized by a wide range of properties. They can be applied in practice and make it possible to model natural biological systems and processes [1–4]. The reaction of metalloporphyrins with peroxides under aerobic conditions can be considered as an analog of one of these processes in the natural systems [2, 4].

The choice of sterically strained metalloporphyrins, including the studied zinc 5,15-di(*ortho*-methyloxyphenyl)-2,3,7,8,12,13,17,18-octamethylporphyrinate (ZnP), is caused by a diversity of their structures and properties.

As it is known, the electronic effects of the substituents and the deformational factor of the macrocycle substantially influence on the properties of porphyrins. The purpose of this work is to study the reactions of ZnP with organic peroxides in *o*-xylene in the presence of imidazole (Im). *o*-Xylene is known to contain a considerable amount of organic peroxides capable of participating in redox transformations [5–8]. The oxidation of ZnP is characterized by the true rate constant (k_v equal to 0.0115 s^{-1} mol^{-1} l. The introduction of the nitrous base changes the structure of the metalloporphyrin and substantially increases k_v.

EXPERIMENTAL

5,15-Di(*ortho*-methyloxyphenyl)-2,3,7,8,12,13,17,18-octamethylporphyrin was synthesized by a standard procedure [9], and its zinc complex ZnP was synthesized according to a described procedure [10]. The UV spectrum of ZnP in benzene is as follows (λ_{max}, nm ($\log\varepsilon$)): 413.9 (5.18), 540 (4.22), 574.4 (4.04). The UV spectrum of ZnP in *o*-xylene is the following (λ_{max}, nm ($\log\varepsilon$)): 410 (5.22), 537 (4.20), 572 (4.02). The UV spectra were recorded on a Specord M 400 instrument.

The concentration of peroxides in *o*-xylene was determined by the photometric method using leucomethylene blue as the indicator [11]. The ZnP concentrations in the working solutions were determined by the molar absorption coefficient ($\log\varepsilon$).

The procedure of studying the complex formation kinetics was documented in detail [12]. The apparent rate constants (k_{app}) for the oxidation of ZnP with peroxides were calculated by a change in the absorbance (A) of the solution at certain time intervals using Eq. (1) of the formally first order under the conditions of an excess of ZnP at the working wavelengths (λ = 537 and 550 nm)

$$k_{app} = 1/\tau \ln(c_0/c_\tau), \quad (1)$$

where c_0 and c_τ are the concentrations of peroxides at the moments 0 and τ.

The k_{app} value was optimized and the root-mean-square deviations were determined by the least-squares method using the Microsoft Excel and ggh.exe (QB-45) programs by the Guggenheim method, which gave the coinciding results. The relative error in k_{app} determination was 3–5%.

Quantum-chemical calculations were performed at the CNDO approximation level [13] by the PM3 semiempirical method [14–16] with the full geometry optimization. The condition for the end of the calculation was a specified gradient of 0.02 kJ mol^{-1} $Å^{-1}$.

RESULTS AND DISCUSSION

The kinetics of ZnP oxidation with organic peroxides (*o*-xylene contains peroxides of the $CH_3C_6H_5CH_2OOH$ and $CH_3C_6H_5CH_2OOCH_3C_6H_5CH_3$ type) was studied at 295 K with the following concentrations of the reactants: $c_{peroxide} = 1.1 \times 10^{-6}$, $c_{ZnP} = 0.69 \times 10^{-5}$–$3.77 \times 10^{-5}$, and $c_{Im} = 4.1 \times 10^{-5}$–$4.1 \times 10^{-3}$ mol/l. The zinc porphyrinate structure is shown below

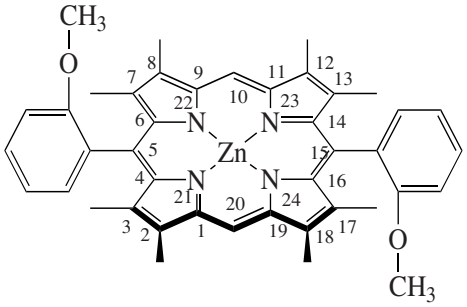

Xylene solutions of ZnP decolorize completely with time in the presence of imidazole (Fig. 1).

Metalloporphyrins can be oxidized at both the central metal atom and periphery [17–19]. The last route is most probable for the complex under study. A decrease in the number of phenyl substituents and the introduction of alkyl groups into the β-position of the macrocycle decrease the aromaticity and, as a consequence, increase the basicity of the complex. Therefore, a possibility to coordinate peroxide by the zinc atom is almost excluded. This is indicated by no changes in the UV spectrum of the oxidized ZnP (Fig. 1).

Two basically different oxidation mechanisms are possible under the experimental conditions. The first mechanism is hydroxylation [16].

It should be mentioned that the introduction of imidazole into the solution (c_{Im} ranges from 10^{-4} to 10^{-3} mol/l) is accompanied by the formation of the (Im)ZnP molecular complex, and this process occurs almost instantly. Thus, the (Im)ZnP complex can participate in the oxidation along with the metalloporphyrin.

The structure and composition of ZnP and the kinetic parameters of the studied reaction changed with the variation of the nitrous base concentration. The UV spectrum of zinc porphyrinate does not substantially change upon the introduction of imidazole in a concentration of 10^{-5} mol/l into the working solution (Fig. 2a). The content of the (Im)ZnP complex in the solution is considerably lower than the ZnP concentration and, hence, the reaction proceeds via the scheme

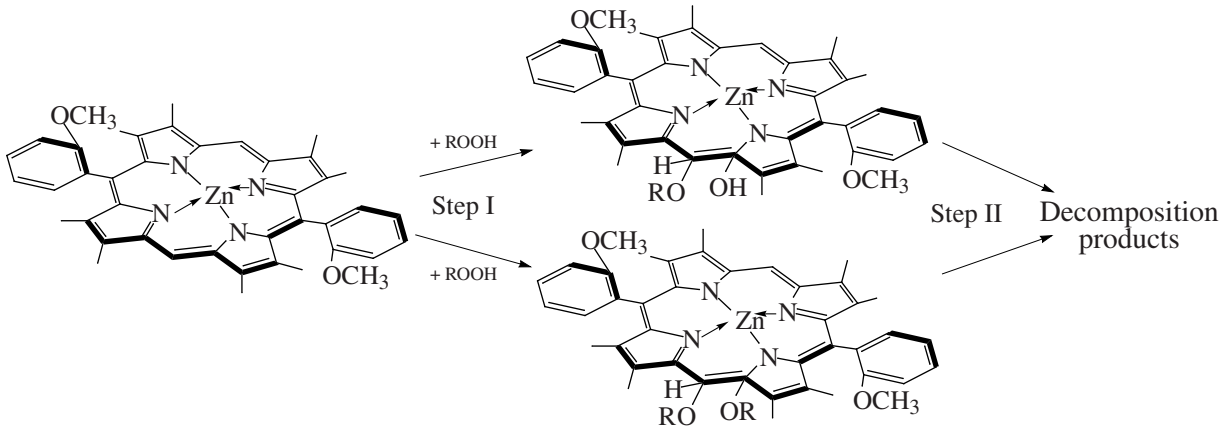

The increase in the imidazole concentration to 10^{-3} mol/l results in the instant transformation of the whole metalloporphyrin into the (Im)ZnP extracomplex. The bathochromic shift of the main absorption bands is 13 nm (Fig. 2c). In this case, the reaction proceeds via the following scheme:

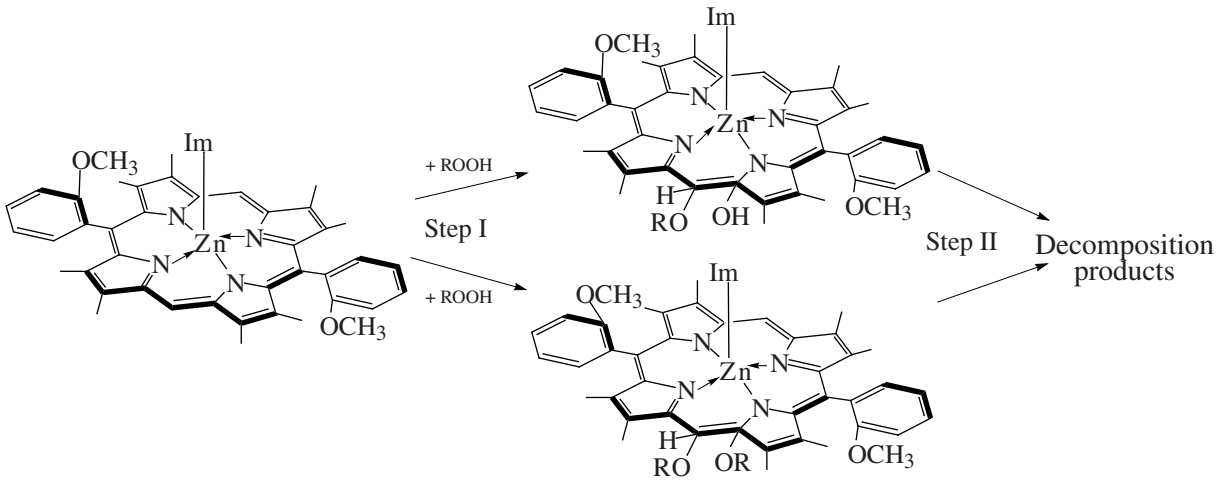

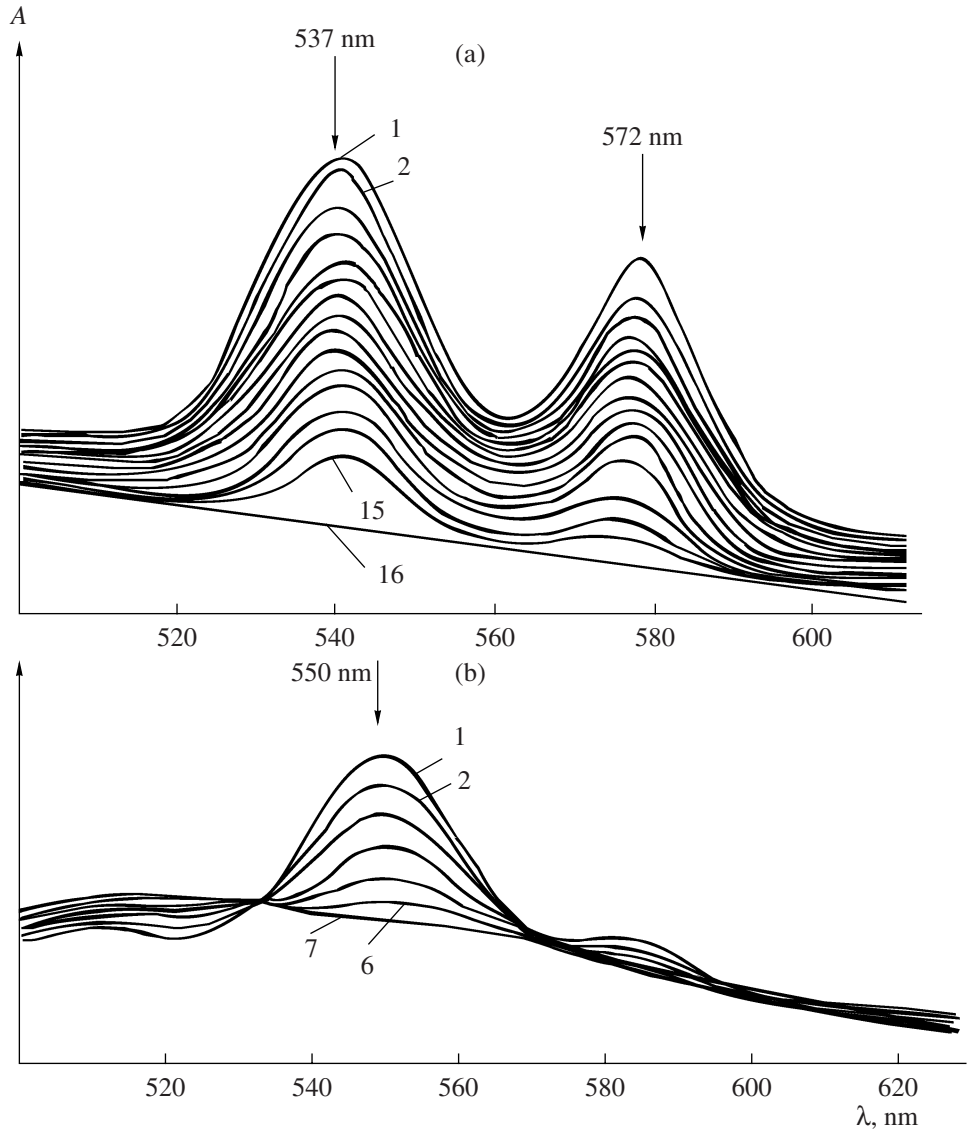

Fig. 1. Changes in the UV spectrum of ZnP during the oxidation in *o*-xylene ($c_{peroxide} = 1.1 \times 10^{-6}$ mol/l) at 295 K in the presence of imidazole: (a) $c_{Im} = 4.1 \times 10^{-5}$ mol/l, $c_{ZnP} = 2.76 \times 10^{-5}$ mol/l, time: (*1*) 0, (*16*) 78.4 h, and (*2–15*) intermediate values; (b) $c_{Im} = 4.1 \times 10^{-3}$ mol/l, $c_{ZnP} = 3.77 \times 10^{-5}$ mol/l, time: (*1*) 0, (*7*) 23.97 h, and (*2–6*) intermediate values.

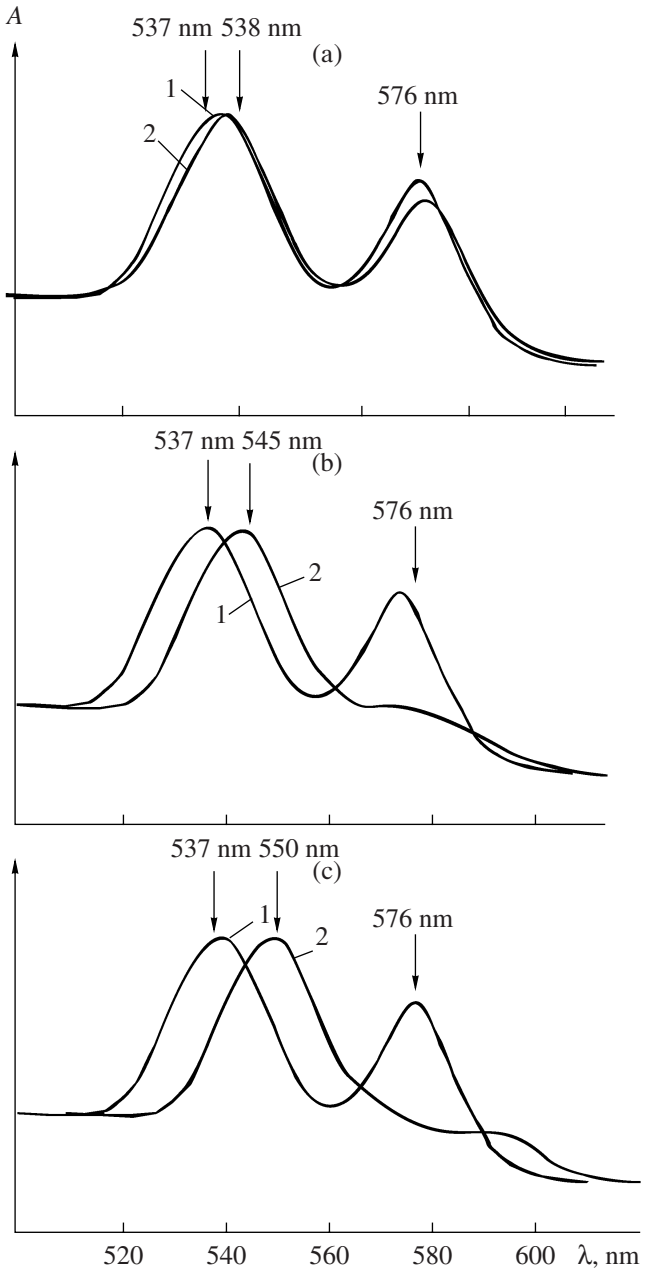

Fig. 2. Changes in the UV spectrum of ZnP upon the introduction into the solution of imidazole in different concentrations: (a) $c_{Im} = 4.1 \times 10^{-5}$, $c_{ZnP} = 2.76 \times 10^{-5}$; (b) $c_{Im} = 4.1 \times 10^{-4}$, $c_{ZnP} = 3.43 \times 10^{-5}$; (c) $c_{Im} = 4.1 \times 10^{-3}$, $c_{ZnP} = 3.77 \times 10^{-5}$ mol/l.

The bathochromic shift of the main absorption bands by ~8 nm is observed in a solution of ZnP in xylene with an imidazole concentration of 10^{-4} mol/l (Fig. 2b), indicating the formation of (Im)ZnP. However, this concentration of the base is insufficient for the whole ZnP to transform into the extracomplex. Therefore, the reaction involving ZnP and (Im)ZnP in parallel occurs in the case.

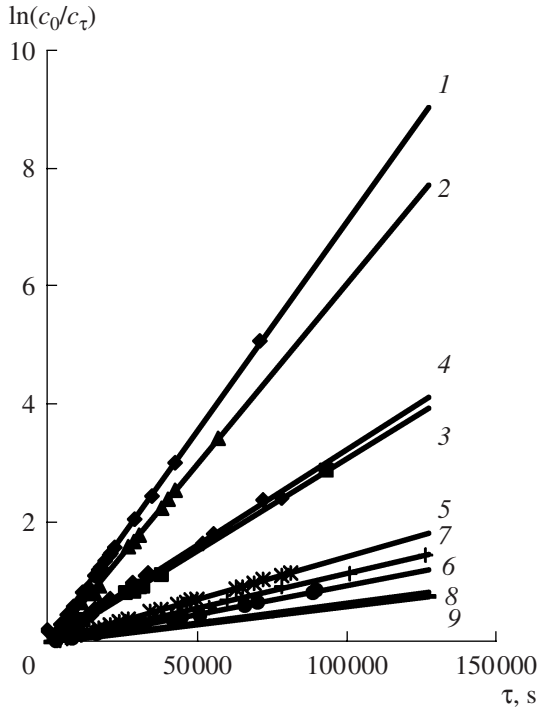

Fig. 3. Plots of $\ln(c_0/c_\tau)$ vs. τ for the oxidation of ZnP with peroxides in *o*-xylene ($c_{peroxide} = 1.1 \times 10^{-6}$ mol/l) at 295 K in the presence of imidazole: $c_{ZnP} = (1)\ 3.77 \times 10^{-5}$, $(2)\ 3.10 \times 10^{-5}$, and $(3)\ 1.3 \times 10^{-5}$ mol/l ($c_{Im} = 4.1 \times 10^{-3}$ mol/l); $c_{ZnP} = (4)\ 3.43 \times 10^{-5}$, $(5)\ 1.50 \times 10^{-5}$, and $(6)\ 0.69 \times 10^{-5}$ mol/l ($c_{Im} = 4.1 \times 10^{-4}$ mol/l); $c_{ZnP} = (7)\ 2.76 \times 10^{-5}$, $(8)\ 1.43 \times 10^{-5}$, and $(9)\ 1.10 \times 10^{-5}$ mol/l ($c_{Im} = 4.1 \times 10^{-5}$ mol/l).

The formation of a bond between the zinc atom and the nitrogen atom of the base ($Zn–N_L$) is accompanied by a change in the electronic and geometric structures of the complex, which results, in turn, in steric strains of the metalloporphyrin macrocycle. The formation of the C–OR and C–OH bonds in both ZnP and (Im)ZnP violates the conjugation in the macrocycle because of the electron density redistribution in the latter. The structural changes appeared in the complex are accompanied by the enhancement of the deformation of the macrocyclic compound. The degree of deformation in (Im)ZnP is greater than that in ZnP. As a result, an unstable sterically strained complex with the open conjugation system is observed and further decomposes to form colorless reaction products (Fig. 1). In this case, step I is rate determining, which is seen in the above presented reaction schemes.

The reaction can also proceed via the free radical mechanism [20]. The activation of peroxide affords radicals of the RO$^\bullet$ and HO$^\bullet$ types interacting with sterically strained zinc porphyrinate and its extracomplex at the *meso*- or α-position to form the radicals: ZnP$^\bullet$(RO), ZnP$^\bullet$(HO), ZnP$^\bullet$ and (Im)ZnP$^\bullet$(RO), (Im)ZnP$^\bullet$(HO), (Im)ZnP$^\bullet$, respectively. The radical

Table 1. Kinetic parameters for the oxidation of ZnP in *o*-xylene in the presence of imidazole ($c_{peroxide} = 1.1 \times 10^{-6}$ mol/l)

$c_{ZnP} \times 10^{-5}$, mol/l	$c_{Im} \times 10^{-3}$, mol/l		
	0.041	0.41	4.1
	$k_{app} \times 10^{-5}$, s^{-1}		
3.77			7.17 ± 0.025
3.43		3.38 ± 0.158	
3.10			6.04 ± 0.144
2.76	1.20 ± 0.045		
1.50		1.48 ± 0.027	
1.43	0.678 ± 0.236		
1.30			2.99 ± 0.419
1.10	0.612 ± 0.006		
0.69		0.959 ± 0.021	
	k_v, s^{-1} mol^{-1} l		
	0.034	0.105	0.296

forms of ZnP and its extracomplex are in the excited state, deformed, and unstable. All this factors result in chromophore destruction (Fig. 1). The formation of the macrocyclic radical is the rate-determining step in this mechanism, and all other steps are faster.

The oxidation of ZnP with peroxides occurred under the pseudo-first-order conditions ($n = 1$) with respect to peroxide, which followed from the rectilinear character of the $\ln(c_0/c_\tau) = f(\tau)$ function and satisfactorily constant k_{app} value (Fig. 3, Table 1)

$$dc_{peroxide}/d\tau = kc^n_{peroxide}. \quad (2)$$

The apparent rate constants for ZnP oxidation increase linearly with an increase in the complex concentration (Fig. 4, Table 1) and are described by the regression equations ($\log k_{app} = 0.8177 \log c_{ZnP} - 0.5294$, $c_{Im} = 4.1 \times 10^{-3}$ mol/l; $\log k_{app} = 0.7879 \log c_{ZnP} - 0.9782$, $c_{Im} = 4.1 \times 10^{-4}$ mol/l; $\log k_{app} = 0.7582 \log c_{ZnP} - 1.4709$, $c_{Im} = 4.1 \times 10^{-5}$ mol/l). These constants concern the slow step of the interaction between the peroxide and the complex rather than the step of macrocycle decomposition.

When the base concentration (4.1×10^{-3} mol/l) is sufficient for the instant transformation of the whole

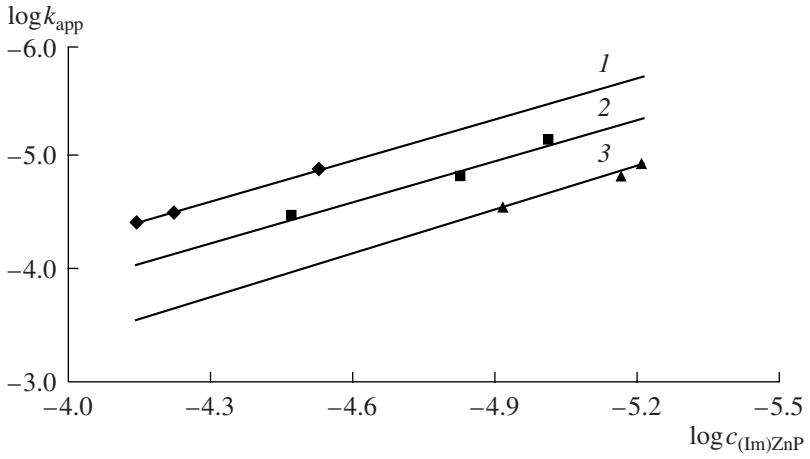

Fig. 4. Plots of the apparent rate constants for ZnP oxidation vs. ZnP concentration in the presence of imidazole at $c_{Im} = (1)$ 4.1×10^{-3}, (2) 4.1×10^{-4}, and (3) 4.1×10^{-5} mol/l ($R^2 = (1)$ 0.981, (2) 0.975, and (3) 0.999).

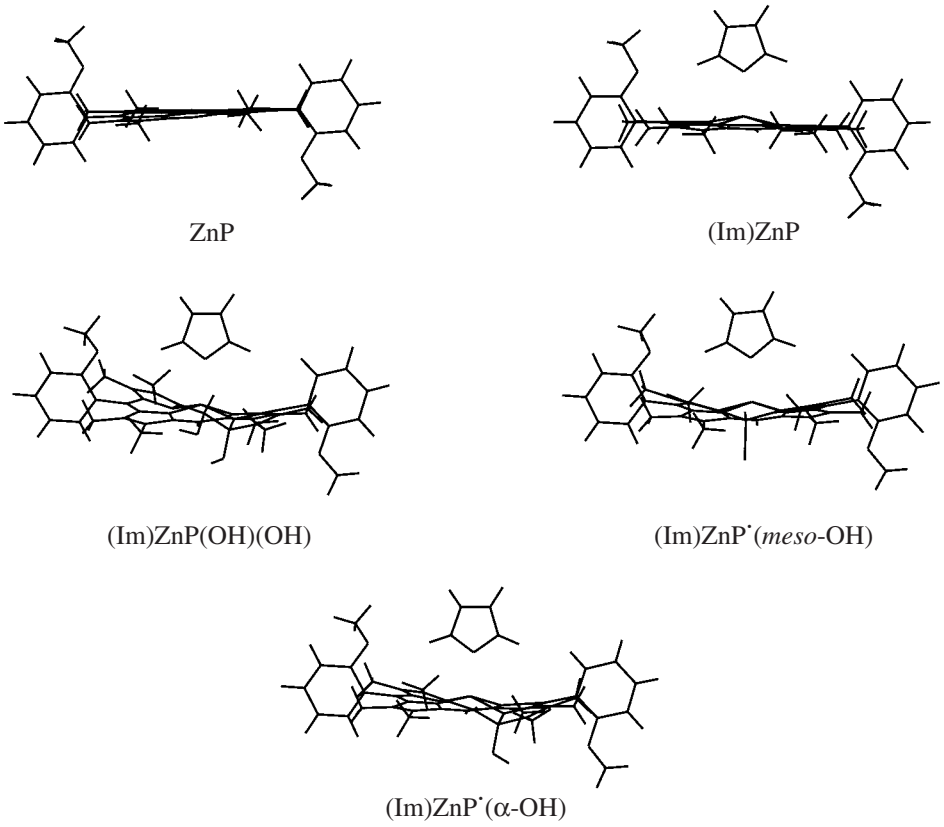

Fig. 5. Structures of ZnP, (Im)ZnP, and selected intermediates in the oxidation of ZnP calculated by the PM3 quantum-chemical method.

ZnP into the extracomplex, the processing of dependence (3) by the least-squares method gave the true rate constant (Table 1), and the reaction order m with respect to [(Im)ZnP] was 0.8177; i.e., $m = 1$ (Fig. 4)

$$\log k_{app} = \log k_v + m \log[(\text{Im})\text{ZnP}]. \quad (3)$$

Thus, the rate equation for this reaction takes the form

$$-dc_{(\text{Im})\text{ZnP}}/d\tau = k_v[(\text{Im})\text{ZnP}][\text{peroxide}]. \quad (4)$$

The comparison of the k_v for a similar reaction involving no imidazole (0.0115 s^{-1} mol^{-1} l) [21] with our data shows that the introduction of the base in a concentration of 4.1×10^{-3} mol/l into the solution increases the oxidation rate by 25 times.

An increase in the imidazole concentration to 4.1×10^{-4} mol/l decreases the reaction rate (Table 1). This is due to the fact that the imidazole molecules can only partially occupy the fifth coordination site. In this case, the oxidation involves both (Im)ZnP and ZnP

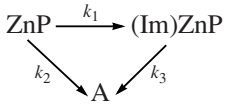

where A are the destruction products of the studied compounds. To write the general kinetic equation for this case, let us consider each step particularly

$$dc_{(\text{Im})\text{ZnP}}/d\tau = k_1[\text{ZnP}] - k_3[(\text{Im})\text{ZnP}], \quad (5)$$

$$dc_A/d\tau = k_2[\text{ZnP}] + k_3[(\text{Im})\text{ZnP}], \quad (6)$$

$$-dc_{\text{ZnP}}/d\tau = dc_{(\text{Im})\text{ZnP}}/d\tau + dc_A/d\tau$$
$$= k_1[\text{ZnP}] - k_3[(\text{Im})\text{ZnP}] \quad (7)$$
$$+ k_2[\text{ZnP}] + k_3[(\text{Im})\text{ZnP}] = [\text{ZnP}](k_1 + k_2).$$

Under our conditions, it is impossible to divide the processes of extracoordination and peroxide oxidation and, therefore, only the overall rate constant $k_v = k_1 + k_2$ was determined (Table 1). The reaction order m with respect to [ZnP] was 0.788 (i.e., $m = 1$) (Fig. 4).

The first order of the reaction with respect to the reactants established in all the cases indicates that the free radicals formed during the oxidation deactivate on the products of metalloporphyrin decomposition.

The data obtained indicate that the presence of imidazole in a solution of ZnP in *o*-xylene substantially increases the reaction rate ($k_v = 0.0115$ s^{-1} mol^{-1} l (without imidazole), $k_v = 0.296$ s^{-1} mol^{-1} l (at $c_{Im} = 10^{-3}$ mol/l)). The change in the imidazole concentration from 4.1×10^{-5}

Table 2. Selected geometric parameters of the sterically strained zinc porphyrin

Complex	Å								deg					
	$Zn–N_{22}$, $Zn–N_{24}$	$Zn–N_{23}$, $Zn–N_{21}$	$N_{22}–N_{24}$, $N_{23}–N_{21}$	Ct–Zn	$Zn–N_L$	$C_{20}–O$, $C_{19}–O$	$C_5–C_{15}$, $C_{10}–C_{20}$	P_{N_4}	$N_{22}ZnN_{23}$, $N_{21}ZnN_{24}$	$N_{22}ZnN_{21}$, $N_{23}ZnN_{24}$	$C_4C_5C_6$, $C_{14}C_{15}C_{16}$	$C_9C_{10}C_{11}$, $C_1C_{20}C_{19}$	$C_{20}C_{19}C_{18}$	$C_{20}C_{19}N_{24}$, $C_{18}C_{19}N_{24}$
ZnP	2.0665	2.0636	4.0873	0.0248			7.1004	11.6033	93.43	86.60	124.27	126.67	122.85	128.09
	2.0211	2.0561	4.1193				6.8202		93.25	86.75	123.57	125.51		109.05
(Im)ZnP	2.1366	2.1037	4.2048	0.3844	2.0979		7.1128	11.6919	91.94	84.70	124.85	127.28	122.96	128.38
	2.1379	2.1101	4.1361				6.8077		91.03	84.63	123.65	125.85		108.65
(Im)ZnP(RO)(OH)[a]	2.0665	2.0503	4.0997	0.5858	2.0813	1.4244	6.9707	11.6363	92.35	87.39	124.41	125.75	110.27	114.32
	2.1975	2.1033	4.0931			1.4083	6.9411		86.77	83.12	123.69	118.41		102.68
(Im)ZnP(RO)(OH)[b]	2.0672	2.0511	4.1245	0.5727	2.0787	1.4261	6.9787	11.6442	92.42	87.51	124.58	125.83	109.67	114.37
	2.2136	2.1027	4.0875			1.4233	6.9572		86.26	83.25	123.82	118.52		102.65
(Im)ZnP(RO)(RO)	2.0352	2.0668	4.3925	0.6255	2.0606	1.4205	7.0469	11.9723	94.05	88.99	124.71	126.30	122.29	127.84
	2.5342	2.0865	4.04832			2.3586	6.9507		85.24	78.57	123.22	114.27		109.82
(Im)ZnP(HO)(OH)	2.0719	2.0492	4.1200	0.5723	2.0833	1.4328	6.9796	11.6474	92.31	87.28	124.55	125.81	110.59	115.93
	2.2043	2.0985	4.0897			1.4106	6.9625		86.93	83.53	123.89	118.89		102.63
$(Im)ZnP^{\bullet}(RO)_m$	2.1139	2.0929	4.1498	0.4369	2.0701	1.4264	7.0619	11.7065	91.06	84.66	124.67	126.11	121.12	129.04
	2.1269	2.1231	4.1299				6.8944		89.19	85.59	125.07	117.15		109.82
$(Im)ZnP^{\bullet}(OH)_m$	2.1112	2.0894	4.1410	0.4333	2.0724	1.4164	7.0548	11.6869	91.28	84.33	124.43	126.19	122.15	127.99
	2.1195	2.1189	4.1252				6.8396		89.54	85.57	125.04	115.54		109.82
$(Im)ZnP^{\bullet}(RO)_\alpha$	2.0666	2.0584	4.1282	0.5677	2.0846		7.0016	11.6258	92.88	86.74	124.27	126.28	110.69	115.07
	2.2151	2.0775	4.0719			1.4342	6.8319		87.59	82.43	123.43	125.97		102.81
$(Im)ZnP^{\bullet}(OH)_\alpha$	2.0640	2.0567	4.1220	0.5613	2.0873		7.0005	11.6248	93.11	86.77	124.37	126.29	111.28	114.44
	2.2083	2.0784	4.0760			1.4175	6.8367		87.88	82.39	123.46	125.78		102.37
$(Im)ZnP^{\bullet}$	2.1366	2.1037	4.2048	0.3841	2.0839		7.1926	11.6622	91.96	82.80	123.87	127.07	129.12	121.45
	2.1376	2.1101	4.1361				6.6535		94.24	83.11	123.93	138.99		109.42

[a] Compound with the OR group in the *meso*-position and the OH groups in the α-position of the macrocycle;
[b] compound with the OR group in the α-position and the OH groups in the *meso*-position of the macrocycle.

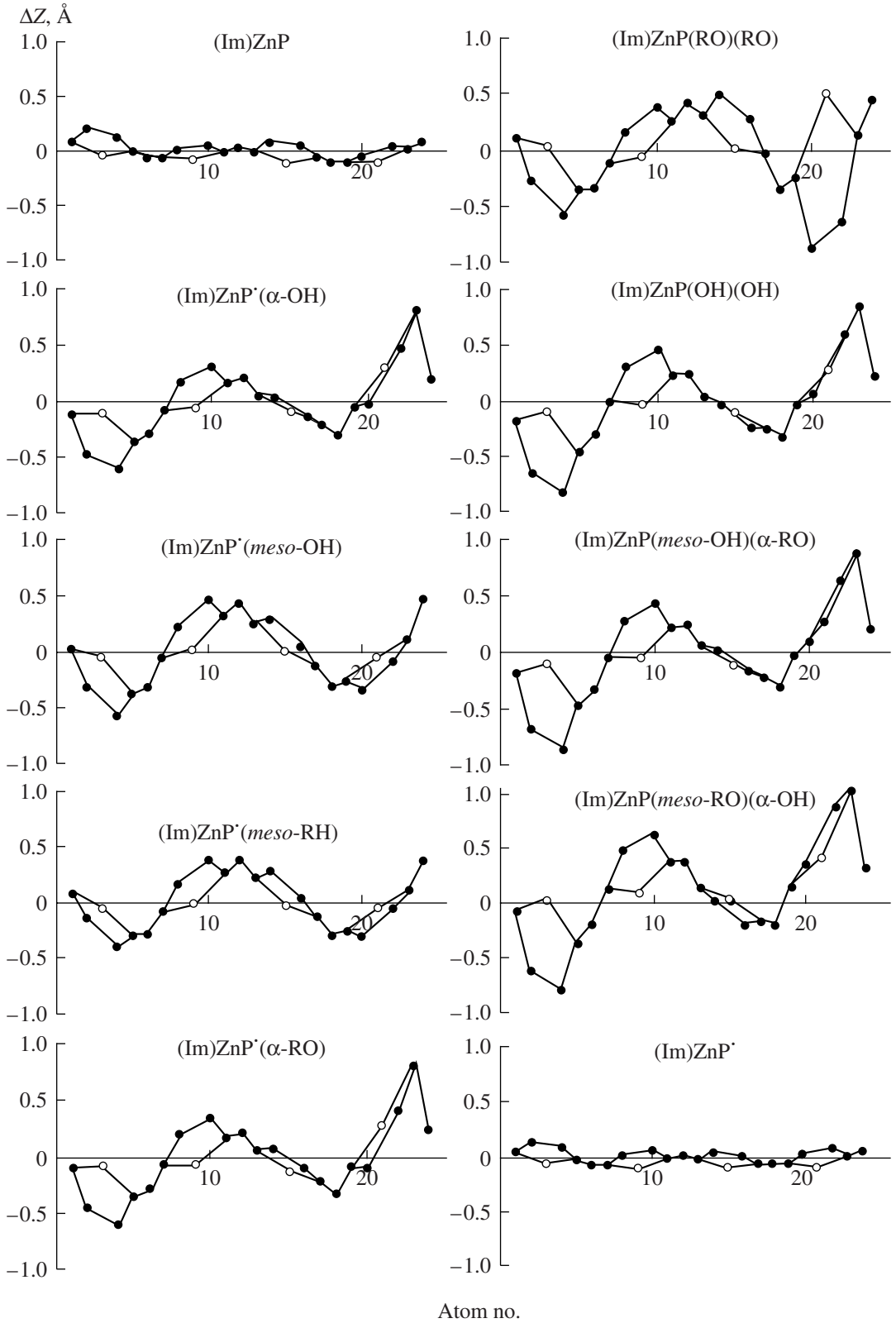

Fig. 6. Deviation from the mean plane of the macrocycle (ΔZ) of the skeletal atoms in the porphyrin macrocycle of (Im)ZnP and the intermediates of the oxidation according to the PM3 quantum-chemical calculation data: ○ are the nitrogen atoms, and ● are the carbon atoms.

to 4.1×10^{-3} mol/l is accompanied by the 8.7-fold change in the reaction rate (Table 1). Under the conditions considered, imidazole is the activator of the oxidation process.

The electronic and geometric structures of zinc porphyrinate and intermediates of the reaction were studied by the PM3 quantum-chemical method. The characteristics of the optimized structures and the molecules of ZnP and its extracomplex (Table 2) indicate the presence of steric strains in the macrocycle of the complex. Comparing the averaged structure of metalloporphyrins having minimal internal strains of the macrocycle [22] with the optimized ZnP molecule, it should be mentioned that the structure of the latter is nonplanar with a fraction of saddle-like deformation and sterically strained [21] (Fig. 5). The planes containing the phenyl substituents form with the N_4 plane an angle of 84°–86°. The OCH_3 groups lie in the plane of the phenyl fragment. The angle of the bond between the carbon atom of phenyl and the methoxy group C_fOC is 117.63°–117.65°. The N_4 plane is parallelogram-shaped with a perimeter(P_{N_4}) of 11.6033 Å.

The formation of the (Im)ZnP complex is accompanied by a change in the electronic and geometric structures of the molecule (Table 2). The degree of macrocycle deformation increases (Figs. 5, 6). The molecule of the zinc porphyrinate extracomplex is strained with a mixed type of deformation: it is cupola-shaped (predominant) with a small fraction of corrugation and saddle. The inclination angle of the phenyl fragment relative to the mean plane of the macrocycle (*XY*) is 88°–89°, and the C_fOC angle is 117.41°–117.62°. The N_4 coordination plane of (Im)ZnP is also parallelogram-shaped. The P_{N_4} value is by 0.0886 Å higher than the perimeter of the ZnP complex.

The structure and the type and degree of deformation in the macrocycle further change substantially during the interaction of the organic peroxide molecule with the (Im)ZnP complex (Table 2; Figs. 5, 6). The sharp enhancement of the saddle-type deformation and an increase in the corrugation are characteristic of (Im)ZnP(*meso*-RO)(α-OH), (Im)ZnP(α-RO)(*meso*-OH), (Im)ZnP(HO)(OH), (Im)ZnP$^{\bullet}$(α-OH), and (Im)ZnP$^{\bullet}$(α-RO). In all the above-mentioned structures, one pyrrole fragment, which is situated near the *meso*-C atom (relative to which the OH or RO group is oriented), deviates substantially from the mean plane of the molecule. For (Im)ZnP(OR)(OR), ((Im)ZnP$^{\bullet}$(*meso*-OH), and (Im)ZnP$^{\bullet}$(*meso*-RO), the corrugation and saddle-like deformation increase slightly against the background of the cupola-shaped deformation (Figs. 5, 6). In the case of (Im)ZnP$^{\bullet}$, torsional deformations are not so substantial, and plane deformations are mainly observed (Table 2, Fig. 6). The decrease in the inclination angle of the phenyl fragments relative to the *XY* plane by 5°–12° and in the C_fOC angle by 1.33°–2.63° are also observed (Table 2). The shift of the zinc atom from the N_4 plane (*Ct*–Zn) increases, and the bond angles and the coordination cavity sizes change (Table 2).

Thus, the presence of the base in the zinc complex changes the electronic and geometric structures of the compound and, as a consequence, the deformation in the compound increases. The formation of the C–OR and C–OH bonds in the macrocycle is accompanied by the further substantial enhancement of steric strains in the molecular complex and, as a result, violates the conjugation and increases the rate of chromophore destruction.

REFERENCES

1. Konovalova, N.V. and Evstigneeva, R.P., *Usp. Khim.*, 2001, vol. 70, no. 11, p. 1059.
2. Evstigneeva, R.P., *Uspekhi khimii porfirinov* (Advances in Porphyrin Chemistry), Golubchikov, O.A., Ed., St. Petersburg: NII khimii SPbGU, 1999, vol. 2., p. 115.
3. Sanders, J.K.M, Bampos, N., Clude-Watson, Z., et al. *The Porphyrin Handbook*, Kadish, K.M., Smith, K.M., and Guilard, R.N.Y., Eds., New York, Academic, 2000, vol. 3, p. 1.
4. Arai, T. and Sato, Y., *Chem. Lett.*, 1990, no. 4, p. 551.
5. Buchler, J.W., Lay, K.L., and Caste, L., *Inorg. Chem.,* 1982, vol. 21, no. 2, p. 842.
6. Juan, L.-Ch. and Bruice, T.C., *J. Am. Chem. Soc.*, 1985, vol. 107, no. 2, p. 512.
7. Kropf, H. and Spangenberg, J., *Liebigs Ann. Chem.*, 1980, no. 12, p. 1923.
8. Dirk, M. and Hambright, P., *J. Chem. Soc., Faraday Trans.*, 1992, vol. 88, no. 14, p. 2013.
9. Mamardashvili, N.Zh., Semeikin, A.S., and Golubchikov, O.A., *Zh. Org. Khim.,* 1993, vol. 29, no. 6, p. 1213.
10. Zaitseva, S.V., Zdanovich, S.A., and Koifman, O.I., *Russ. J. Phys. Chem.*, 2005, vol. 79, p. 45.
11. *Comprehensive Organic Chemistry*, Barton, D.H. and Ollis, W.D., Eds., Oxford: Pergamon, 1979, vol. 2.
12. *Eksperimental'nye metody khimicheskoi kinetiki* (Experimental Methods of Chemical Kinetics), Emanuel', N.M. and Sergeev, G.B., Eds., Moscow: Vysshaya Shkola, 1980.
13. Bersuker, I.B., *Elektronnoe stroenie i svoistva koordinatsionnykh soedinenii* (Electronic Structure and Properties of Coordination Compounds), Leningrad: Khimiya, 1986.
14. Schidt, M.W., Baldridge, K.K., Boatz, J.A. et al., *J. Comput. Chem.*, 1993, vol. 14, no. 11, p. 1347.
15. Stewart, J.J., P, *J. Comput. Aided Mol. Des.*, 1990, vol. 4, no. 1, p. 1.
16. Fletcher, R., *Methods of Optimization*, New York: Wiley, 1980, p. 45.
17. Liston, D.J. and West, B.O., *Inorg. Chem.,* 1985, vol. 24, no. 10, p. 1568.

18. Berezin, B.D. and Sennikova, G.V., *Kinet. Katal.*, 1968, vol. 9, no. 3, p. 528.
19. Kalish, H., Camp, J.E., Stepien, M., et al., *J. Am. Chem. Soc.*, 2001, vol. 123, no. 47, p. 11719.
20. Bagdasaryan, Kh.S., *Teoriya radikal'noi polimerizatsii* (Radical Polymerization Theory), Moscow: Nauka, 1966.
21. Simonova, O.R., Zaitseva, S.V., and Koifman, O.I., Abstracts of Papers *XXIX nauch. sessii Ros. seminara po khimii porfirinov i ikh analogov "Dostizheniya i perspektivy razvitiya koordinatsionnoi khimii porfirinov. Itogi 50-letnikh issledovanii"* (XXIX Scientific Session of the Russian Seminar on the Chemistry of Porphyrins and Their Analogs "Achievements and Prospects of the Development of the Porphyrin Coordination Chemistry. Results of 50-year Studies") Ivanovo, 2006, p. 84.
22. Hoard, J.L., *Ann N.Y. Acad. Sci,* 1973, vol. 206, no. 1, p. 18.